Australian Meteorological and Oceanographic Journal 63 (2013) 365–376

Global simulations of the impact on contemporary climate of a perturbation to the sea-to-air flux of dimethylsulfide

Albert J. Gabric[1], Bo Qu[2], Leon Rotstayn[3,4] and Jill M. Shephard[5]
[1]School of Environment, Griffith University, Nathan, Queensland, Australia
[2]Science Department, Nantong University, China
[3]CSIRO Marine and Atmospheric Research, Aspendale, Victoria, Australia
[4]The Centre for Australian Weather and Climate Research,
a partnership between CSIRO and the Bureau of Meteorology, Australia
[5]School of Biological Sciences and Biotechnology, Faculty of Science and Engineering,
Murdoch University, Murdoch, Western Australia, Australia

(Manuscript received April 2012; revised March 2013)

The sea-to-air flux of the biogenic sulfur (S) compound dimethylsulfide (DMS) is thought to constitute an important radiative impact on climate, especially in remote marine areas. Previous biogeochemical modelling analyses simulate medium to large changes in the sea-to-air flux of DMS in polar regions under warming scenarios. Here we assess the global radiative impact of such a prescribed change in DMS flux on contemporary climate using a low-resolution atmospheric general circulation model. This impact operates through the atmospheric oxidation of DMS to radiatively-active sulfate aerosols, which are known to both reflect incoming short-wave radiation and to affect the microphysical properties of clouds, for example, through an increase in cloud albedo. We use an atmospheric GCM with incorporated sulfur cycle, coupled to a mixed-layer ('q-flux') ocean, to estimate the climatic response to a prescribed meridionally-variable change in zonal DMS flux, as simulated in a previous modelling analysis. We compare baseline sulfur emissions (contemporary anthropogenic S and contemporary DMS sea-to-air flux), with contemporary anthropogenic S and a perturbed DMS flux. Our results indicate that the global mean DMS vertically integrated concentration increases by about 41 per cent. The relative increase in DMS annual emission is around 17 per cent in 70–80°N, although the most significant increase is in 50–70°S, up to 70 per cent. However, concentrations of atmospheric SO_2 and SO_4^{2-} increase by only about eight per cent. The oxidation of DMS by OH increases by about 20 per cent. Oxidation of SO_2 to SO_4^{2} by H_2O_2 increases seven per cent. The oxidation of SO_2 by O_3 increases around six per cent. Overall sulfur emissions increase globally by around 4.6 per cent.

Global mean aerosol optical depth (AOD) increases by 3.5 per cent. Global mean surface temperature decreases by 0.6 K. There is a notable difference between the impacts in the southern and northern hemispheres. In general, most processes and chemical species related to the sulfur cycle show a larger increase in the southern hemisphere, except SO_2 and the oxidation of DMS by NO_3. The global mean direct radiative forcing due to the DMS change is –0.05 Wm^{-2} with total forcing (direct + indirect effects) of –0.48 Wm^{-2}. This perturbation on DMS flux leads to a mean surface temperature decrease in the southern hemisphere of around 0.8 K, compared with a decrease of 0.4 K in the northern hemisphere.

Corresponding author address: A. Gabric, School of Environment, Griffith University, Nathan QLD 4111. Email: ajgabric@gmail.com.

Introduction

Aerosols, from both anthropogenic and natural sources, affect planetary albedo both indirectly, by forming cloud condensation nuclei (CCN) and increasing cloud-top albedo, and directly, by backscattering incoming solar radiation. As the global radiation budget is sensitive to the amount of cloud and their reflectivity of solar radiation, CCN, on which cloud droplets can form, play a critical role in the earth's radiative balance and in the sensitivity of climate to increasing greenhouse gas (GHG) emissions. A recent evaluation of the amount of warming in the industrial age suggests that GHG forcing of climate has been partially offset by increased concentrations of atmospheric aerosols (Schwartz et al. 2010). Indeed, modelling estimates suggest the adoption of stricter air pollution control strategies that focus on the reduction of anthropogenic aerosol emissions will lead (by 2030) to a global annual mean equilibrium temperature response of 2.18 K, compared with increasing GHG concentrations alone that leads to a temperature response of 1.20 K (Kloster et al. 2010). Thus, the future emission of aerosols constitutes one of the largest uncertainties in projections of anthropogenic climate change (Anderson et al. 2003, Bender 2012).

The natural marine aerosol comprises two distinct types: those emitted as primary particles, viz. sea-salt and organic aerosols produced by wave and wind-driven mechanical disruption of the ocean surface, and those formed in the atmosphere by gas-to-particle conversion (as secondary particles) e.g. non-sea-salt (nss) sulfate and other organic species (Twomey 1991). Mechanical generation results in the production of aerosol particles with radii typically ranging from 0.1 to 100 micron or more, while gas-to-particle conversion through processes such as binary homogeneous nucleation, heterogeneous nucleation and condensation, results in the formation of new particles typically nanometers in size (Bigg 2007).

Dimethylsulfide (DMS) is a volatile, biogenic sulfur compound emanating from the oceans and one of the key sources of natural aerosol over the remote ocean (Bates et al. 1992, Gondwe et al. 2003). DMS is produced from dimethylsulphoniopropionate (DMSP), a compound synthesised by marine phytoplankton. A link between DMS, sulfate aerosols and global climate was first hypothesised by Shaw (1983), and elaborated on by Charlson et al. (1987). It was suggested that warming of the oceans would increase the algal production of DMS, which, after ventilation to the atmosphere and oxidation reactions would lead to an increase in sulfate aerosol, more CCN, and brighter clouds, thus cooling the earth's surface, and providing a negative feedback on the warming impact of greenhouse gas emissions. This proposition, later called the CLAW hypothesis, has subsequently stimulated a very large and ongoing research effort (Ayers and Cainey 2007). Several large scale studies inspired by the International Global Atmospheric Chemistry program (IGAC) have addressed aspects of the DMS-aerosol-climate connection, including the Atlantic Stratocumulus Transition Experiment/Marine Aerosol Gas Exchange (ASTEX/MAGE) (Huebert et al. 1996), the Aerosol Characterization Experiment (ACE-1) (Bates et al. 1998), and the Arctic Ocean Experiment (AOE-91) (Leck et al. 1996).

Over the last two decades key parts of the CLAW hypothesis have been corroborated empirically. These include the observed coherence between a DMS oxidation product methanesulphonic acid (MSA) and CCN (Ayers and Gras 1991), and the link between aerosol nucleation and the marine cycle of DMS (Clarke et al. 1998). Satellite data and global sulfur transport models have also confirmed the role of DMS as a source of CCN and sulfate aerosols over the remote oceans, particularly in the southern hemisphere, where anthropogenic emissions of sulfur are comparatively low (Vallina et al. 2006). A link between solar radiation and DMS production has recently been suggested as another possible facet of the DMS-climate feedback, whereby a decrease in cloudiness would promote DMS emissions (Vallina and Simo 2007).

However, parts of the CLAW hypothesis have been challenged; in particular the role of DMS oxidation products in the formation of CCN in the marine boundary layer has been debated and remains controversial, with often conflicting results reported in the literature (O'Dowd et al. 1999, Pirjola et al. 2000, Korhonen et al. 2008). Indeed in a recent review, Quinn and Bates (2011) provocatively argue that the CLAW hypothesis should now be retired due to a lack of strong evidence for a connection between DMS emissions and CCN production. However, not all researchers are as keen to consign the CLAW hypothesis to the scientific wastebasket. In a major review of aerosols and climate published just a little before than that of Quinn and Bates, Carslaw et al. (2010) include a lengthy discussion of the CLAW hypothesis and emphasise the need for more data in several key areas.

It is, however, becoming clear that the atmospheric chemistry of DMS is more complex than envisaged in the CLAW hypothesis, and that a host of other marine biogenic compounds may also contribute to the formation of secondary aerosols, including iodine and isoprene (Liss et al. 1997) and other biogenic organics. For example, marine microgels (in dissolved organic matter released by phytoplankton) have been identified as a dominant CCN source in the high Arctic (Orellana et al. 2011). Intriguingly however, DMS, through its oxidation by-product sulfuric acid, is thought to be a determinant of the size distribution of these Arctic microgels, and hence their efficacy as sources of CCN (Orellana et al., 2011)

The synthesis and biogeochemical cycling of DMS and its precursor DMSP involves the entire marine microbial community, including both autotrophs and heterotrophs and their complex interactions and is still not completely understood (Belviso et al. 2004). It is also being appreciated that DMS concentration is linked to the physical state of the upper ocean, resulting from a complex interplay of vertical

mixing and light dependent photolysis (Gabric et al. 1993, Gabric et al. 2008). This complexity has been a limiting factor in developing robust parameterisations between DMS and easily measureable upper ocean parameters (Anderson et al. 2001, Simó and Dachs 2002).

Climate change leading to ocean warming and acidification will undoubtedly alter various aspects of the marine food web (Parmesan 2006, Hopkins et al. 2010), and thus also affect DMS production, but the magnitude and direction of change is as yet unclear. It is noteworthy that the climatically important sea-to-air flux of DMS seems to be a minor sink (less than ten per cent) in the overall oceanic cycle of DMS under current climatic conditions (Malin 1997), suggesting the potential for quite large changes in the future. However, various global scale modelling experiments over the last decade suggest the magnitude of the DMS flux change under warming is still uncertain, although most studies indicate an overall increase in flux in line with the original CLAW hypothesis (Bopp et al. 2003, Gabric et al. 2004, Gunson et al. 2006, Kloster et al. 2007, Vallina et al. 2007, Cameron-Smith et al. 2011).

Regional modelling studies that have calibrated the DMS production model to local field data in the Antarctic and the Arctic Ocean simulate large increases (25–80 per cent) in the DMS sea-to-air flux under enhanced greenhouse conditions (Gabric et al. 2003, Gabric et al. 2005). The special role played by polar regions has also been confirmed in a global modelling analysis (Gabric et al. 2004), where the greatest perturbation to the DMS flux was simulated at high latitudes in both hemispheres, with little change predicted in the tropics and sub-tropics. The largest change in annual mean flux (+106 per cent) was simulated in the southern hemisphere between 50–60°S (Gabric et al. 2004).

It is clear that the projected impact of warming on DMS emissions is spatially variable, and likely to be especially influenced by changes in the polar oceans. It is not clear how such a perturbation in the DMS flux, and the resulting change to the atmospheric S burden in the polar atmospheres, may affect regional temperature patterns or the overall radiative balance of the planet. It is known, however, that the polar regions display an asymmetric response to warming, with the Arctic warming accelerated due to the sea-ice albedo feedback effect (Anderson et al. 2006, Serreze and Francis 2006). Recent suggestions of large-scale geo-engineering of the planet via injections of sulfate aerosols to the lower stratosphere make the current analysis especially timely (Rasch et al. 2008, Vaughan and Lenton 2011).

To investigate the overall radiative impact of such a prescribed latitudinally-variable increase in DMS flux, we employ an atmospheric general circulation model (AGCM) with a sulfur atmospheric chemistry component that includes a DMS sea-to-air flux parameterisation. We have perturbed the global contemporary DMS flux field according to the simulated relative 10° zonal changes derived in previous DMS modelling analyses under tripled CO_{2e} conditions, (Gabric et al. 2004, Gabric et al. 2005) and investigated the sensitivity of contemporary climate to such a perturbation. Our analysis considers effects on contemporary climate of an increase in the atmospheric burden of DMS and its oxidation by-products; however we do not consider associated impacts of warming on atmospheric chemistry, which could significantly alter DMS atmospheric oxidation rates, and is beyond the scope of the present study.

Methods

Atmospheric circulation model

The atmospheric model used in this study is a low-resolution (spectral R21) version of the Mk3 CSIRO atmospheric GCM described by Gordon et al. (2002). This low-resolution version has 18 hybrid vertical levels and a horizontal resolution of approximately 5.6 degrees in longitude and 3.2 degrees in latitude. A detailed description of the model structure is given by Rotstayn and Lohmann (2002). The model has been augmented with a comprehensive treatment of the tropospheric sulfur (S) cycle and other aerosol components and includes an updated radiation code described in Rotstayn et al. (2007). The model's treatment of air-sea fluxes in sea-ice regions is described in O'Farrell (1998).

Prognostic variables in the S-cycle model are dimethylsulfide (DMS), sulfur dioxide (SO_2) and sulfate, with S chemistry following that given in the ECHAM4 model (Feichter et al. 1996). Carbonaceous aerosol and mineral dust emission are included using the prescriptions by Cooke et al. (1999) and Ginoux et al. (2004), respectively. The formation of sea salt aerosol is a function of 10 m wind speed above the ocean surface (O'Dowd et al. 1997), with sea salt aerosol assumed to be well mixed in the marine boundary layer, and set to zero above the boundary layer (Jones et al. 2001). Large-scale wet scavenging is linked to the warm rain and frozen precipitation processes in the stratiform cloud microphysical scheme (Rotstayn 1997) and the convection scheme (Gregory and Rowntree 1990). Below-cloud scavenging and in-cloud scavenging are as described by (Rotstayn and Lohmann 2002) .

Cloud droplet number concentrations (cm^{-3}) over oceans (Nocean) and land (Nland) were estimated using a slightly modified version of the relationships given by Menon at al. (2002),

$$N_{ocean} = 10^{2.41+0.5log(SO_4)+0.13log(OM)+0.05log(SS)} \quad ...(1)$$

and

$$N_{land} = 10^{2.41+0.5log(SO_4)+0.13log(OM)} \quad ...(2)$$

where SO_4, OM and SS are the mass concentrations of sulfate, particulate organic matter and sea salt, respectively in $\mu g\ m^{-3}$. We reduced the coefficient that multiplies SO_4 in Eqn 2 from 0.50 to 0.26, a value that was obtained from extensive observations in an earlier study (Boucher and Lohmann 1995); see Rotstayn et al. (2007) for further discussion of the reasons for this change.

Specific aspects of the S model and chemistry are

described in the following. DMS and SO_2 are oxidised by reaction with the hydroxyl (OH) radical during the day and DMS also reacts with the nitrate radical (NO_3) at night. Both oxidants are prescribed as three dimensional monthly mean fields. It is assumed that the only end product of DMS oxidation is SO_2, thus ignoring the relatively small yield of methanesulphonic acid (MSA) and other oxidation products. Following the suggestion that an additional (unknown) oxidant is required to obtain reasonable agreement between observed and modelled DMS concentrations (Chin et al. 1996, James et al. 2000), we increase the reaction rate between DMS and OH by a factor of two, relative to the original rate given by Hynes et al (1986). This is smaller than the factor of 3.3 needed by James et al. (2000) to enable their model to reproduce measurements at Mace Head Research Station in Ireland.

In the aqueous phase, SO_2 reacts with hydrogen peroxide (H_2O_2) and ozone (O_3) to form sulfate. The amount of SO_2 dissolved in cloud water is calculated according to Henry's Law. The reaction rates and the effective Henry's law constant for SO_2 are calculated assuming that aqueous phase equilibria and electroneutrality are maintained. Since the distribution of H_2O_2 is prescribed, the model may tend to overestimate the SO_2 oxidation rate in regions where H_2O_2 is depleted by the reaction with SO_2. The aqueous-phase chemistry is applied inside the liquid-water part of stratiform clouds and inside convective clouds up to the freezing level. More details on the model's treatment of aqueous phase S chemistry are given in Rotstayn and Lohmann (2002) .

Sulfur emissions are identical to those used in ECHAM4 (Lohmann et al. 1999), except for the treatment of DMS emission from the ocean surface. Biogenic sources of sulfur in the model include SO_2 from non-eruptive volcanoes, amounting to 8.0 Tg S yr^{-1} (Spiro et al. 1992, Graf et al. 1997), and emissions of DMS from oceans, soils and plants. Emissions of DMS from soils and plants follow Spiro et al. (1992), and amount to 0.9 Tg S yr^{-1}. The concentration of DMS in seawater is taken from the database of Kettle et al. (1999), with updates described by Kettle and Andreae (2000). The sea-to-air flux of DMS is calculated using a parameterisation derived by Nightingale et al. (2000). A recently compiled DMS global database (Lana et al. 2011) indicates that annual global DMS emissions are larger than previously thought, 28.1 Tg S yr^{-1} or 17 per cent higher than estimated by Kettle and Andreae (2000). This is largely due to better observational coverage of DMS at high latitudes in the last decade.

The model's treatment of sea ice (O'Farrell 1998) allows a fraction of open water to remain at all times at grid points where sea ice exists. At these grid points, emission of DMS is calculated only for the areas of open water. With this treatment, the annually averaged emission of DMS from the ocean surface in the control (baseline) run described below is 22.1 Tg S yr^{-1}.

Anthropogenic sources of sulfur are fossil fuel use and smelting (66.7 Tg S yr^{-1}) (Benkovitz et al. 1996) , and biomass burning (2.5 Tg S yr^{-1}) (Hao et al. 1990). These emissions occur as SO_2, except that three per cent of the emissions from fossil fuel and smelting are assumed to occur as sulfate. This feature is not included in ECHAM4. According to Benkovitz et al. (1996), between 1.4 per cent and five per cent of the total anthropogenic emissions occur as sulfate. The anthropogenic emissions from Benkovitz et al. (1996) are for the year 1985, and include a substantial seasonal cycle for Europe, with winter SO_2 emissions set roughly 25 per cent higher than the annual mean, and summer emissions set roughly 25 per cent lower than the annual mean. Since 1995, sulfur emissions have increased over Asia and decreased over Europe and North America e.g. Smith et al. (2001).

The model's skill in reproducing observations of the atmospheric burden of DMS, SO_2 and sulfate was comprehensively discussed by Rotstayn and Lohmann (2002). The model shows better agreement with the observations over Europe (where it agrees to within a factor of two) than over North America, where it shows a positive bias in all quantities. Over oceanic points in the southern hemisphere, the model is in reasonable agreement with the observations. This is important for the present analysis as the Southern Ocean is where the simulated change in DMS emission due to warming is most significant (Gabric et al. 2004). Over the Antarctic continent, the modelled sulfate concentration is almost twice the observed value, while the wet deposition at the South Pole is smaller than that observed, suggesting that the model underestimates wet deposition in this region.

Numerical experiments

We performed several simulations in which the atmospheric GCM was run coupled to a mixed layer ('q flux') ocean model. The mixed layer ocean (MLO) model assumes a mixed layer depth of 50 m in regions away from the sea ice, increasing to 150 m under sea ice. The monthly mean oceanic heat transports used in these runs were calculated using the method of Watterson et al. (1997) from a ten-year run of the atmospheric GCM forced by prescribed SSTs.

To establish a baseline data set a control run (baseline: run labeled B) was performed with input forcings and anthropogenic and natural sulfur sources representative of the contemporary climate of the late 20th century. The GCM was run for both 40 and 50 year simulation times to check the model's approach to equilibrium. As there were only minor differences between the two integrations, the first 30 years of this run were used as a spin-up step to allow the model to achieve quasi-equilibrium. Data were then obtained as averages for each parameter from the final ten-year period of the 40-year simulation.

In the flux perturbation experiment (modified: run labeled M), the baseline DMS zonal flux was perturbed in ten degree latitude bands between 70°N and 70°S according to the results of the global modelling analysis of Gabric et al. (2004), which used the Simo and Dachs (2002) parameterisation between DMS concentration, chlorophyll-a and mixed layer depth. For the high Arctic (70–80°N) we used the

results from an analysis using a regionally calibrated DMS production model by Gabric et al. (2005). Both these previous studies used the IPCC/ISP92a radiative forcing scenario and simulated the change in DMS flux that would occur under tripled CO_{2e} conditions. The flux perturbations represent the change in mean annual flux and thus do not resolve seasonal variability (see Table 1).

In both experiments, data were collected as averages from the final ten years of the simulation. The GCM output variables were compared both at the global level and averaged over each hemisphere. Data were collected for 11 parameters describing the atmospheric distribution of sulfur species and their reactions, as well as aerosol optical depth (AOD), and surface temperature. In some instances the variables were averaged over several latitude bands.

Results and discussion

Figure 1 shows the mean relative increase in DMS annual emission from baseline to modified simulations by latitude. The peak change (+44 per cent) occurs around 60°S. In the northern hemisphere, the Arctic Ocean shows a significant increase (+33 per cent), especially at higher latitudes. DMS annual emission increased significantly in the southern hemisphere (especially between 50–70°S) and in the Arctic Ocean (70–80°N). Comparing baseline and modified simulations, the relative increase in DMS annual emission in the 50–60°S band reached over 70 per cent, while in 70–80°N, DMS annual emission increased 16.7 per cent.

The global and hemispheric mean changes in various sulfur variables and reactions between the baseline and the modified simulations are given in Table 2 and Figs 2 and 3.

Table 1. Applied Perturbation to DMS flux for modified (M) simulation (Gabric et al. 2004).

Band	*Applied Perturbation to annual zonal DMS Flux (%)*
80–70°N	86
70–60°N	19.5
60–50°N	28.9
50–40°N	–2.2
40–30°N	2.2
30–20°N	-3.6
20–10°N	5.5
10–0°N	–7.2
0–10°S	3.7
10–20°S	5.9
20–30°S	6.5
30–40°S	10.7
40–50°S	32.3
50–60°S	106.9
60–70°S	46.3
70–80°S	None applied

Almost all aerosol-related fields have a higher increase in the southern hemisphere, except SO_2 and DMN (oxidation of DMS by NO_3).

The DMS flux perturbation leads to the vertically integrated DMS concentration increasing by almost 50 per cent in the southern hemisphere, and just under ten per cent in the northern hemisphere. The oxidation of DMS by OH

Fig. 1. Relative increase in annual emission of DMS by latitude.

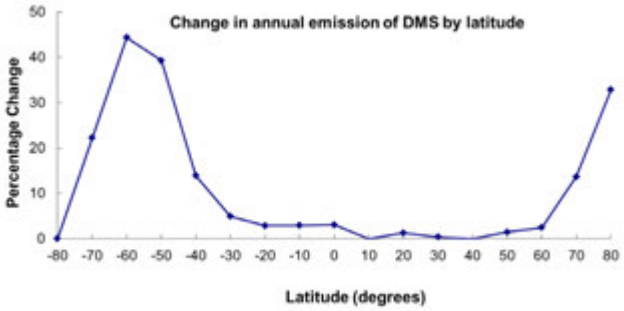

Fig. 2. Global mean and hemispheric change for various parameters and processes between the baseline (B) and the modified (M) simulations. For definition of acronyms see Table 2.

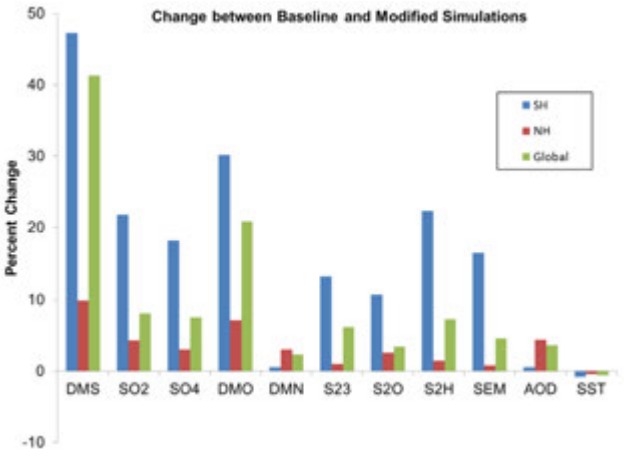

Fig. 3. Seasonal change in DMS atmospheric burden between baseline (B) and modified (M) simulations for the southern hemisphere and northern hemisphere.

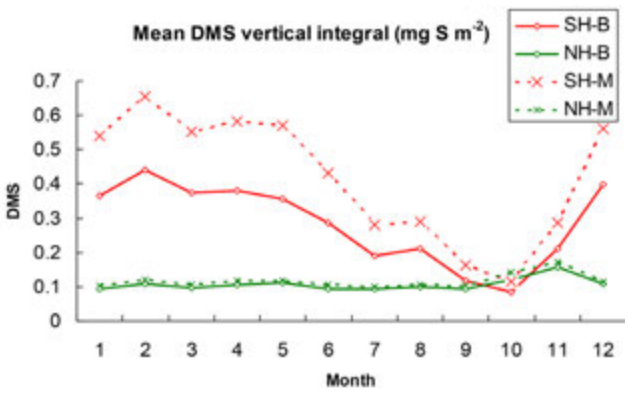

Table 2. Mean value and change (%) for various parameters and processes between baseline and modified simulations.

Model parameter or process (acronym)	*Run*	*Global Mean*		*Southern hemisphere mean*		*Northern hemisphere Mean*	
DMS vertical integral ($mgSm^{-2}$) **(DMS)**	B	0.19	+41.3%	0.28	+47.3%	0.11	+9.9%
	M	0.28		0.42		0.12	
Sulfur dioxide vertical integral ($mgS\ m^{-2}$) **(SO_2)**	B	0.66	+8.1%	0.34	+21.8%	0.98	+4.3%
	M	0.72		0.41		1.02	
Sulfate vertical integral ($mgS\ m^{-2}$) **(SO_4)**	B	1.34	+7.5%	0.78	+18.4%	1.89	+3.0%
	M	1.44		0.93		1.95	
Oxidation of DMS by OH ($10^{-12}kgm^{-2}s^{-1}$) **(DMO)**	B	1.23	+20.8%	1.47	+30.2%	1.0	+7.1%
	M	1.49		1.91		1.07	
Oxidation of SO_2 by O_3 ($10^{-12}kgm^{-2}s^{-1}$) **(S23)**	B	0.47	+6.2%	0.39	+13.3%	0.54	+1.0%
	M	0.50		0.45		0.55	
Oxidation of DMS by NO_3 ($10^{-12}kgm^{-2}s^{-1}$) **(DMN)**	B	0.159	+2.3%	0.0948	+0.54%	0.22	+3.1%
	M	0.162		0.0953		0.23	
Oxidation of SO_2 to SO_4 by OH ($10^{-12}kgm^{-2}s^{-1}$) **(S2O)**	B	0.60	+3.4%	0.28	+10.7%	0.92	+2.6%
	M	0.62		0.31		0.93	
Oxidation of SO_2 to SO_4 by H_2O_2 ($10^{-12}kgm^{-2}s^{-1}$) **(S2H)**	B	1.93	+7.3%	1.07	+22.3%	2.78	+1.4%
	M	2.07		1.31		2.83	
Sulfur emissions ($10^{-12}kgm^{-2}s^{-1}$) **(SEM)**	B	5.72	+4.6%	2.72	+16.6%	8.73	+0.8%
	M	5.98		3.17		8.80	
Aerosol Optical Depth at 550 nm **(AOD)**	B	0.10	+3.5%	0.087	+0%	0.12	+1.7%
	M	0.11		0.087		0.13	
Surface temp. (K) **(SST)**	B	286.9	–0.6 K	286.5	–0.8 K	287.3	–0.4 K
	M	286.3		285.7		286.9	

increases about 21 per cent and a little more than two per cent via reaction with NO_3. However, the DMS oxidation by-products SO_2 by SO_4 only increase globally by about eight per cent. The oxidation of SO_2 by O_3 increases around 6.2 per cent. The oxidation of SO_2 to sulfate by OH increases 3.4 per cent, while oxidation of SO_2 to sulfate by H_2O_2 increases 7.3 per cent. Global sulfur emissions increase 4.6 per cent with most of the change occurring in the southern hemisphere.

In the northern hemisphere, the DMS atmospheric burden is fairly constant throughout the year (Fig. 3). A similar data pattern has also been noted by various other authors (Smith et al. 2001, Rotstayn and Lohmann 2002, Andreae et al. 2003). In the southern hemisphere the DMS cycle is seasonal with very high concentrations during the austral summer (Curran and Jones 2000) reaching an annual maximum in February, with a minimum during the austral spring in October. DMS concentration increases around 46 per cent in the austral summer and 54 per cent in the austral autumn.

Comparing Figs 4 and 5, there is little change in DMS and SO_2 in the northern hemisphere, but more change in the southern hemisphere, especially in the early part of the year. Unlike DMS, SO_2 and sulfate are higher in the northern hemisphere than southern hemisphere (Fig. 4(a,b)) due to anthropogenic emissions, although the simulated change is greater in the southern hemisphere. In the northern hemisphere, the anthropogenic burden reaches a minimum in July due to higher oxidative efficiency to form nss-sulfate (Chin et al. 2000, Rotstayn and Lohmann 2002).

Figure 5 shows the change in column-integrated summertime DMS between baseline and modified simulations for the southern hemisphere (upper two panels) and northern hemisphere (lower two panels). The region with highest DMS concentration is over the Southern Ocean between 45–65°S, where the annual mean DMS increased 45 per cent from 0.25 mgS m^{-2} to 0.33 mgS m^{-2}; monthly mean during summer (January–March) DMS increased 28 per cent in this region (from 0.30 mgS m^{-2} to 0.39 mgS m^{-2}). In the northern hemisphere, the most significant increase in DMS occurred in the Arctic Ocean with high DMS concentrations also over remote regions of North Atlantic Ocean and North Pacific Ocean (Fig. 5(c)).

The seasonal change in rate of oxidation of DMS by OH is given in Fig. 6(a). The mean oxidation rate increases 30 per cent in the southern hemisphere and 7.1 per cent in the northern hemisphere with a seasonal variation that mirrors that in DMS in both hemispheres. There is higher DMS oxidative removal during summertime in both hemispheres. There is a significant increase in the rate of oxidation of SO_2 to sulfate by H_2O_2 in late summer in southern hemisphere (around 32 per cent increase in January–March. see Fig. 6(b)), while increased oxidation of SO_2 to sulfate by OH is around 14.7 per cent in the southern hemisphere, but only

Fig. 4. (a) Mean change in SO_2 atmospheric burden for baseline (B) and modified (M) simulations in the southern hemisphere and northern hemisphere. (b) Mean change in SO_4 atmospheric burden for baseline (B) and modified (M) simulations in the southern hemisphere and northern hemisphere.

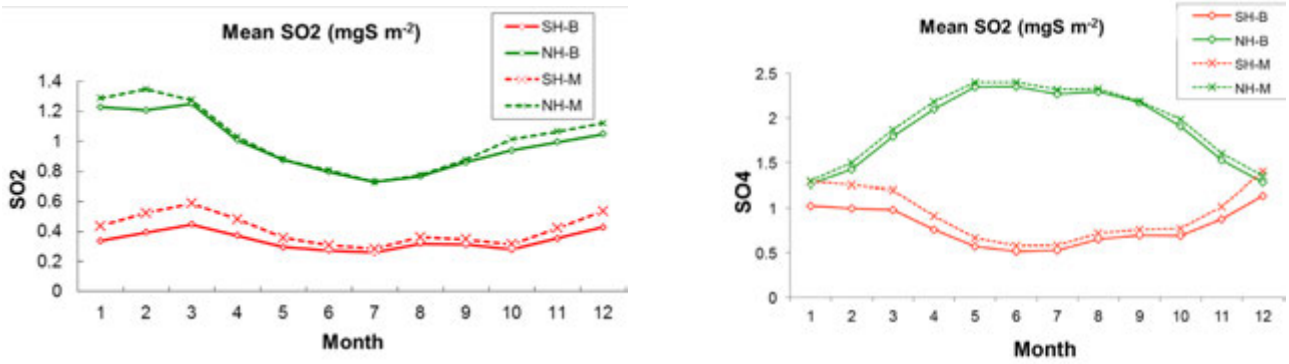

Fig. 5. Change in spatial distribution of summertime DMS ($mgSm^{-2}$) for baseline (B) and modified (M) simulations (a) southern hemisphere modified (Jan–Mar); (b) southern hemisphere baseline (Jan–Mar); (c) northern hemisphere modified (Jun–Aug); (d) northern hemisphere baseline (Jun–Aug).

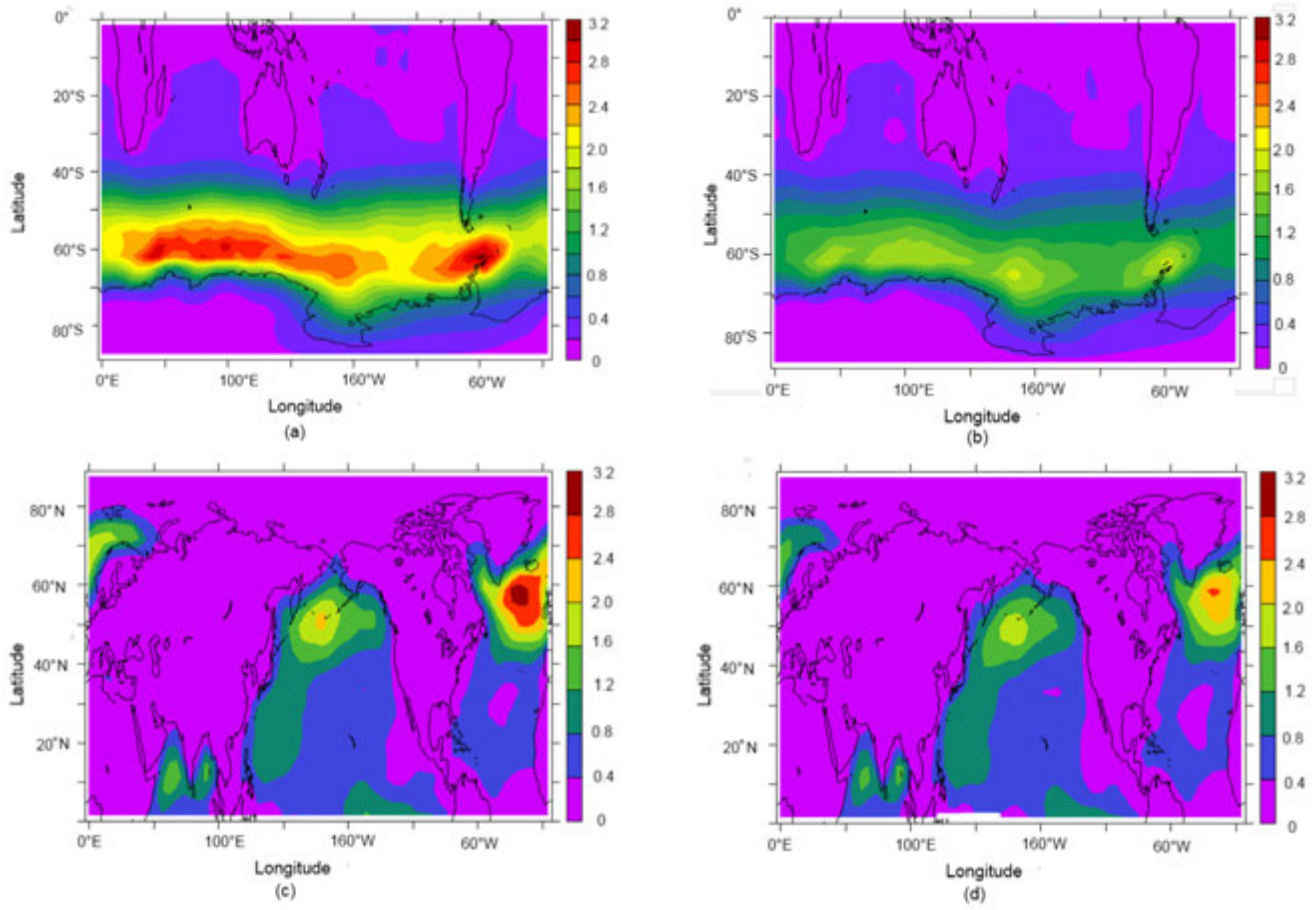

one per cent in the northern hemisphere.

The global mean change in aerosol optical depth (AOD) at 550 nm for the baseline and the modified simulations is 3.6 per cent (Fig. 2). This figure is relatively small, as AOD has a substantial component from natural aerosols such as mineral dust and sea salt, and anthropogenic emissions of carbonaceous aerosols (Tsigaridis et al. 2006). The variation of AOD is seasonal, with summertime maxima in both hemispheres (not shown). Gabric et al. (2002) found a correlation between summer AOD and chlorophyll in the Southern Ocean, which suggested an influence of DMS-derived aerosols on AOD was possible.

Global mean surface temperature decreases 0.6 K mainly due to the increased emissions of DMS and SO_2 leading to

Fig. 6. Mean DMO (left) and S2H (right) comparisons between baseline (B) and modified (M) simulations for the southern hemisphere and northern hemisphere.

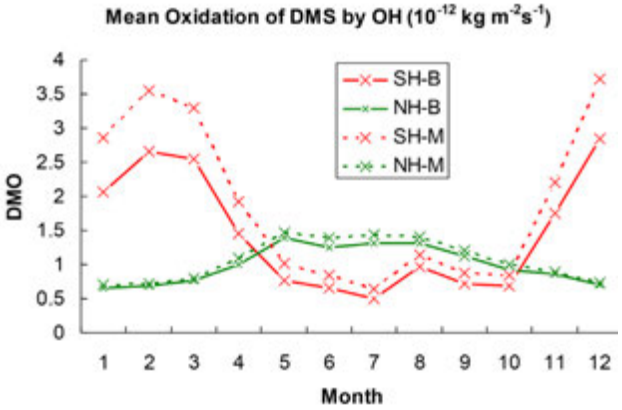

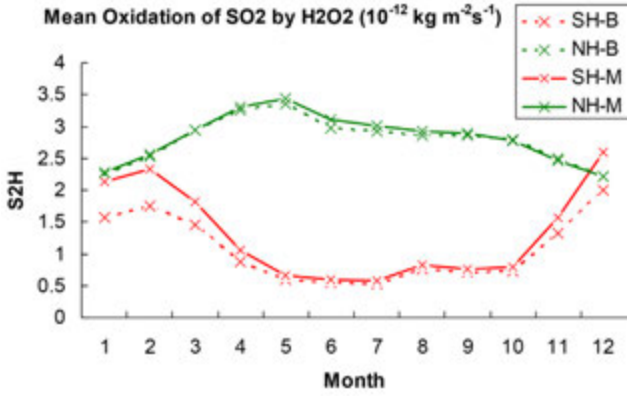

Fig. 7. Change in mean surface temperature for modified (M) and baseline (B) simulations for the southern hemisphere and northern hemisphere.

Fig. 8. Global SST change by latitude from baseline (B) to modified (M) simulations.

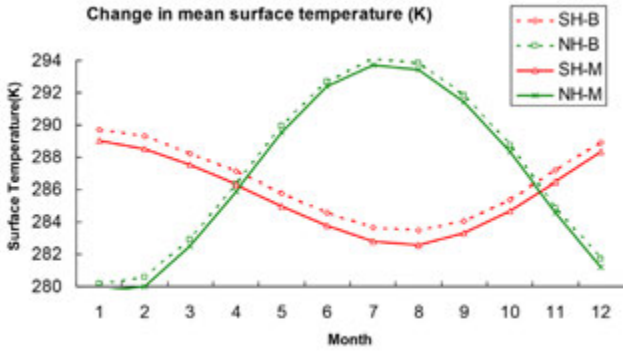

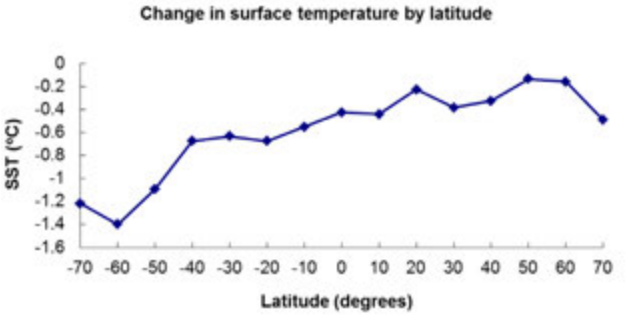

an increased burden of radiatively active sulfate (Figs 8 and 9). However, there are quite large hemispheric differences in the temperature reduction, with the southern hemisphere cooling more (0.77 K for the southern hemisphere versus 0.42 K for the northern hemisphere). This change is due to a combination of direct aerosol forcing, and indirect aerosol effects (increases of cloud albedo and lifetime).

The total and direct radiative forcing due to the DMS change has been calculated and the zonal means are shown in Fig. 9. The total radiative forcing is estimated as a 'radiative flux perturbation' (Lohmann et al. 2010), namely the difference in the radiative flux at the top of the atmosphere between two simulations that are similar to baseline and modified, except that SSTs are prescribed to follow a climatological annual cycle. The global mean radiative forcing due to the direct effect is –0.05 Wm^{-2}, with a total of –0.48 Wm^{-2}. The total radiative flux perturbation, which accounts for changes in cloud albedo and lifetime as well as direct effects, is a little noisy (causing some values to be slightly above zero) because the method allows the changes in cloud lifetime to feed back on the meteorology.

Clearly, the dominant effect in our runs is the indirect effect, especially over the Southern Ocean. The clouds in the southern hemisphere will be very susceptible to changes in sulfate, which induce increases in cloud droplet number concentration (CDNC), starting from a low base, because the air there is unpolluted. Table 3 shows the simulated change of CDNC. Global mean CDNC increased 3.6 per cent. For the southern hemisphere, mean CDNC increased 11 per cent but decreased 0.68 per cent in the northern hemisphere.

Due to differences in the atmospheric sulfur cycle treatment in various global atmospheric models, and more importantly, the varying parameterisation of the marine sulfur biogeochemistry, a direct comparison with previous modelling estimates of the climate sensitivity to a change in DMS flux is problematic. It is nevertheless interesting to compare our results with other studies. For example, Bopp et al. (2004) simulate the impact on radiative forcing of a DMS flux perturbation associated with a doubling of preindustrial CO_2 (cf. our study where we analyse the impact under tripled CO_2). Their results indicate a significant change in forcing only in the mid-latitudes of the southern hemisphere during summer, similar to –1.5 Wm^{-2}, but little change elsewhere. Bopp et al. (2004) do not estimate the resulting temperature change, however their overall radiative forcing results are broadly consistent with ours.

Gunson et al. (2006) examine the climate sensitivity to an instantaneous doubling and halving of global

Fig. 9. Total and direct radiative forcing due to the DMS change along latitude.

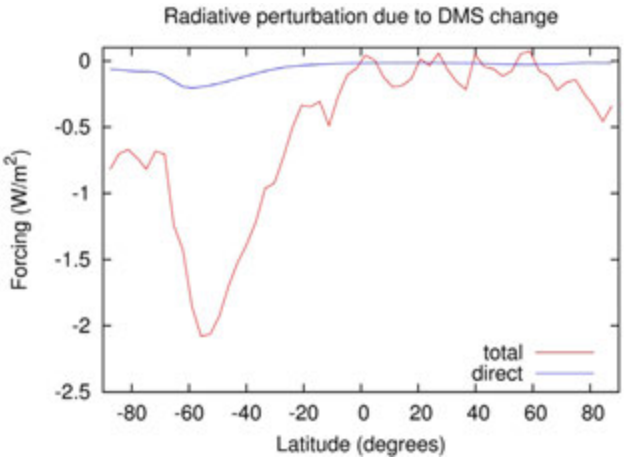

mean DMS flux (no latitudinal variability in the flux perturbation was included). For a doubled DMS flux, which is only partly comparable to our study, Gunson et al. (2006) simulate a change in cloud radiative forcing of –1.8 Wm^{-2} and a global surface temperature decrease of about 0.8 K. Interestingly, these global mean values are quite similar to those presented here where we apply a meridionally-variable DMS flux perturbation.

In marked contrast, Kloster et al. (2007) simulate conditions for tripled CO_2, and find the global DMS flux is reduced by ten per cent. The DMS atmospheric burden is reduced by only three per cent, owing to a longer lifetime of DMS in the atmosphere in a warmer climate (+7 per cent). The largest reduction in the DMS sea surface concentration is simulated in the Southern Ocean (–40 per cent).

More recently, Cameron-Smith et al. (2011), use a state-of-the-art GCM with embedded biogeochemistry to simulate the changes in zonal averaged DMS flux for tripled CO_2 conditions, and report an increase of over 150 per cent in the Southern Ocean. Although they did not examining the climate sensitivity, the simulation of a marked future increase in the southern hemisphere DMS flux supports our assumptions. However, their simulated perturbation is even higher than the DMS flux perturbations applied in our study, suggesting the possibility that our analysis may underestimate the climate sensitivity to future changes in DMS emissions.

Conclusion

We used a low-resolution (spectral R21) version of the Mk3 CSIRO atmospheric GCM, with incorporated sulfur cycle, to estimate the global radiative impact of a prescribed meridionally-variable change in zonal average DMS flux. In the modified simulation the global mean DMS atmospheric concentration increases around 41 per cent. The relative increase in DMS annual emission is around 17 per cent in 70–80°N with the most significant increase of almost 70 per cent occurring in the southern hemisphere, between 50°S and 70°S. However, the DMS oxidation by-products, SO_2 and sulfate increase just over eight per cent. The oxidation of DMS by OH increases about 21 per cent. The oxidation of SO_2 by O_3 increases around 6.2 per cent. Oxidation of SO_2 by H_2O_2 increases by 30 per cent in the austral summer (DJF) in the southern hemisphere.

Table 3. Change in CDNC (droplets/cm^3) from baseline (B) to modified (M) simulations.

Latitude	*Southern hemisphere*		*Northern hemisphere*		*Global*	
	B	*M*	*B*	*M*	*B*	*M*
Mean	110.4	122.4	192.2	190.9	151.3	156.7
% change	+10.9%		–0.68%		+3.6%	
S.D.	59.65	58.04	106.9	105.2	95.76	91.61
Minimum	1.32	1.55	17.61	23.62	1.32	1.55
Maximum	403.1	375.8	796.0	850.1	796.0	850.1

The direct and total radiative forcing due to the DMS change was –0.05 Wm^{-2} and –0.48 Wm^{-2}, respectively. We found that most quantities related to the sulfur cycle show a higher increase in the southern hemisphere, except SO_2 and oxidation of DMS by NO_3. Generally, the perturbation of DMS flux leads to a higher atmospheric burden of related sulfur species, especially in the southern hemisphere. Interestingly, even for a relatively modest increase of global DMS average emissions (+4.6 per cent), surface temperature is simulated to decrease by around 0.8 K in the southern hemisphere and by 0.4 K in the northern hemisphere. Due to the different GCMs and biogeochemical models employed these results are not directly comparable with previous estimates of the climate sensitivity to a change in DMS flux. However, it is interesting to note that the analysis by Cameron-Smith et al. (2011) suggests our results may be a lower bound on the climate sensitivity to future increases in DMS emissions, especially in the southern hemisphere.

Sea ice plays a dominant role in determining the intensity of the DMS fluxes in the Arctic and Antarctic and to a large extent determines the climate sensitivity of both regions (Gabric et al. 2005, Jones et al. 2010). Although the projected loss of sea-ice was included in our analysis of the perturbation to DMS flux, recent research suggests that the nexus between sea-ice and DMS emissions is more complex than previously thought (Qu and Gabric 2010, Asher et al. 2011). An outstanding challenge is to better understand the impact of sea-ice ice melting on DMS flux variation in the zonal average, and to evaluate the impact of this source of DMS on the radiative budget. Our results support the hypothesis that a warming-induced increase of biogenic sulfate will have a modest but not insignificant impact on global mean temperatures with strong hemispheric asymmetry. It is likely that changes in biogenic sulfur emissions from the oceans will need to be incorporated into the next phase of earth

system models to more accurately project future climate change.

Acknowledgments

We are grateful for the efforts of colleagues who are responsible for the development of the CSIRO climate model. We also gratefully acknowledge the financial assistance of an ASAC Grant from the Australian Antarctic Division.

References

Anderson, P., Bermike, O., Bigelow, N., Brigham-Grette, J., Duvall, M., Edwards, M. and Velichko, A. 2006. Last Interglacial Arctic warmth confirms polar amplification of climate change. *Quaternary Science Reviews, 25,* 1383–400.

Anderson, T.L., Charlson, R.J., Schwartz, S.E., Knutti, R., Boucher, O., Rodhe H. and Heintzenberg, J. 2003. Climate forcing by aerosols – a hazy picture. *Sci., 300,* 1103–4.

Anderson, T.R., Spall, S.A., Yool, A., Cipollini, P., Challenor, P.G., and Fasham, M.J.R. 2001. Global fields of sea surface dimethylsulfide predicted from chlorophyll, nutrients and light. *Journal of Marine Systems, 30,* 1–20, DOI: 10.1016/s0924-7963(01)00028-8.

Andreae, M.O., Andreae, T.W., Meyerdierks, D. and Thiel, C. 2003. Marine sulfur cycling and the atmospheric aerosol over the springtime North Atlantic. *Chemosphere, 52,* 1321–43.

Asher, E.C., Dacey, J.W.H., Mills, M.M., Arrigo, K.R. and Tortell, P.D. 2011. High concentrations and turnover rates of DMS, DMSP and DMSO in Antarctic sea ice. *Geophys. Res. Lett., 38,* DOI: L23609/10.1029/2011gl049712.

Ayers, G.P. and Cainey, J.M. 2007. The CLAW hypothesis: a review of the major developments. *Environmental Chemistry, 4,* 366–74, DOI: 10.1071/en07080.

Ayers, G.P. and Gras, J.L. 1991. Seasonal relationship between cloud condensation nuclei and aerosol methanosulphonate in marine air. *Nature, 353,* 834–5.

Bates, T.S., Lamb, B.K., Guenther, A., Dignon, J. and Stoiber, R.E. 1992. Sulfur emissions to the atmosphere from natural sources. *J. Atmos. Chem., 14,* 325–37.

Bates, T.S., Huebert, B.J., Gras, J.L., Griffiths, F.B. and Durkee, P.A. 1998. International Global Atmospheric Chemistry (IGAC) Project's First Aerosol Characterization Experiment (ACE-1): Overview. *J. Geophys. Res., 103,* 16297–318.

Belviso, S., Bopp, L., Moulin, C., Orr, J.C. Anderson, T.R., Aumont, O., and Simo, R. 2004. Comparison of global climatological maps of sea surface dimethyl sulfide. *Global Biogeochemical Cycles, 18.*

Bender, F.A.M. 2012. Aerosol Forcing: Rapporteur's Report and Summary. *Surveys in Geophysics, 33,* 693–700 DOI: 10.1007/s10712-011-9160-0.

Benkovitz, C., Scholtz, M., Pacyna, J., Tarrason, L., Dignon, J., Voldner, E. and Graedel, T. 1996. Global gridded inventories of anthropogenic emissions of sulfur and nitrogen. *J. Geophys. Res., 99,* 20725–56.

Bigg, E.K. 2007. Sources, nature and influence on climate of marine airborne particles. *Environmental Chemistry, 4,* 155–61.

Bopp, L., Aumont, O., Belviso, S. and Monfray, P. 2003. Potential impact of climate change on marine dimethyl sulfide emissions. *Tellus Series B–Chemical and Physical Meteorology, 55,* 11–22.

Bopp, L., Boucher, O., Aumont, O., Belviso, S., Dufresne, J.L., Pham, M. and Monfray, P. 2004. Will marine dimethylsulfide emissions amplify or alleviate global warming? A model study. *Canadian Journal of Fisheries and Aquatic Sciences, 61,* 826–35.

Boucher, O. and Lohmann, U. 1995. The sulfate-CCN-cloud albedo effect. A sensitivity study with two general circulation models. *Tellus (B), 47,* 281–300.

Cameron-Smith, P., Elliott, S., Maltrud, M., Erickson, D. and Wingenter, O. 2011. Changes in dimethyl sulfide oceanic distribution due to climate change. *Geophys. Res. Lett., 38,* DOI: 10.1029/2011gl047069.

Carslaw, K.S., Boucher, O., Spracklen, D.V., Mann, G.W., Rae, J.G.L., Woodward, S. and Kulmala, M. 2010. A review of natural aerosol interactions and feedbacks within the Earth system. *Atmospheric Chemistry and Physics, 10,* 1701–37, DOI: 10.5194/acp-10-1701-2010.

Charlson, R.J., Lovelock, J.E., Andreae, M.O. and Warren, S.G. 1987. Oceanic phytoplankton, atmospheric sulphur, cloud albedo and climate. *Nature, 326,* 655–61.

Chin, M., Jacob, D.J., Gardner, G.M., Foreman-Fowler, M.S., Spiro, P.A. and Savoie, D.L. 1996. A global three-dimensional model of tropospheric sulfate. *J. Geophys. Res., 101,* 18667–690.

Chin, M., Rood, R.B., Lin, S.J., Muller, J.F. and Thompson, A.M. 2000. Atmospheric sulfur cycle simulated in the global model GOCART: Model description and global properties. *J. Geophys. Res. Atmos., 105,* 24671–87, DOI: 10.1029/2000jd900384.

Clarke, A.D., Davis, D., Kapustin, V.N., Eisele, F. Chen, G., Paluch, I., and Albercook, C. 1998. Particle nucleation in the tropical boundary layer and its coupling to marine sulfur sources. *Science, 282,* 89–92.

Cooke, W.F., Liousse, C., Cachier, H. and Feichter, J. 1999. Construction of a 1 degrees x 1 degrees fossil fuel emission data set for carbonaceous aerosol and implementation and radiative impact in the ECHAM4 model. *J. Geophys. Res. Atmos., 104,* 22137–62.

Curran, M.A.J. and Jones, G.B. 2000. Dimethyl sulfide in the Southern Ocean: seasonality and flux. *J. Geophys. Res., 105,* 20451–9.

Feichter, J., Kjellstrom, E., Rodhe, H., Dentener, F., Lelieveld, J. and Roelofs, G.-J. 1996. Simulation of the tropospheric sulfur cycle in a global climate model. *Atmos. Environ., 30,* 1693–707.

Gabric, A.J., Cropp, R., Ayers, G.P., McTainsh, G., and Braddock, R. 2002. Coupling between cycles of phytoplankton biomass and aerosol optical depth as derived from SeaWiFS time series in the Subantarctic Southern Ocean. *Geophys. Res. Lett., 29,* DOI: 1112 10.1029/2001gl013545.

Gabric, A.J., Cropp, R., Hirst, A., and Marchant, H. 2003. The sensitivity of dimethylsulphide production to simulated climate change in the eastern Antarctic Southern Ocean. *Tellus 55B,* 966–81.

Gabric, A.J., Matrai, P.A., Kiene, R.P., Cropp, R., Dacey, J.W.H., DiTullio, G.R., and Slezak, D. 2008. Factors determining the vertical profile of dimethylsulfide in the Sargasso Sea during summer. *Deep-Sea Research Part II – Topical Studies in Oceanography, 55,* 1505–18, DOI: 10.1016/j.dsr2.2008.02.002.

Gabric, A.J., Murray, C.N., Stone, L., and Kohl, M. 1993. Modeling the production of dimethylsulphide during a phytoplankton bloom. *J. Geophys. Res., 98,* 22805–16.

Gabric, A.J., Qu, B., Matrai, P.A., and Hirst, A.C. 2005. The simulated response of dimethylsulfide production in the Arctic Ocean to global warming. *Tellus B, 57,* 391–403.

Gabric, A.J., Simo, R., Cropp, R.A., Hirst, A.C., and Dachs, J. 2004. Modeling estimates of the global emission of dimethylsulfide under enhanced greenhouse conditions – art. no. GB2014. *Global Biogeochemical Cycles, 18,* B2014.

Ginoux, P., Prospero, J.M., Torres, O., and Chin, M. 2004. Long-term simulation of global dust distribution with the GOCART model: correlation with North Atlantic Oscillation. *Environmental Modelling and Software, 19,* 113–28.

Gondwe, M., Krol, M., Gieskes, W., Klaassen, W., and de Baar, H. 2003. The contribution of ocean-leaving DMS to the global atmospheric burdens of DMS, MSA, SO_2, and NSS SO_4^{2-} – art. no. 1056. *Global Biogeochemical Cycles, 17,* 1056.

Gordon, H.B., Rotstayn, L.D., McGregor, J.L., Dix, M.R., Kowalczyk, E.A., O'Farrell, S.P., and Elliott, T. I. 2002. The CSIRO Mk3 Climate System Model. *CSIRO Atmospheric Research Technical Paper 60,* 134.

Graf, H., Feichter, J., and Langmann, B. 1997. Volcanic sulfur emissions: Estimates of source strength and its contribution to the global sulfate distribution. *J. Geophys. Res., 102,* 10727–38.

Gregory, D. and Rowntree, P.R. 1990. A mass flux convection scheme with representation of cloud ensemble characteristics and stability-dependent closure. *Mon. Weather Rev., 118,* 1493–506.

Gunson, J.R., Spall, S.A., Anderson, T.R., Jones, A., Totterdell, I.J., and Woodage, M.J. 2006. Climate sensitivity to ocean dimethylsulphide emissions. *Geophys. Res. Lett., 33,* DOI: L07701 Artn l07701.

Hao, W., Liu, M., and Crutzen, P.J. 1990. Estimates of annual and regional releases of CO_2 and other trace gases to the atmosphere from fires in the tropics, based on the FAO statistics for the period 1975–1980. *Fire in the Tropical Biota. Ecosystem Processes and Global Challenges.*

J. Goldammer. New York, Springer-Verlag: 440–62.

Hopkins, F.E., Turner, S.M., Nightingale, P.D., Steinke, M., Bakker, D., and Liss, P.S. 2010. Ocean acidification and marine trace gas emissions. *Proceedings of the National Academy of Sciences of the United States of America, 107,* 760–5, DOI: 10.1073/pnas.0907163107.

Huebert, B.J., Pszenny, A., and Blomquist, B. 1996. The ASTEX/MAGE experiment. *J. Geophys. Res. Atmos., 101,* 4319–29.

Hynes, A.J., Wine, P.H., and Semmes, D.J. 1986. Kinetics and mechanisms of OH reactions with organic sulfides. *J. Phys. Chem., 90,* 4148–56.

James, J.D., Harrison, R.M., Savage, N.H., Allen, A.G., Grenfell, J.L., Allan, B.J., and Robertson, L. 2000. Quasi-Lagrangian investigation into dimethyl sulfide oxidation in maritime air using a combination of measurements and model. *J. Geophys. Res., 105,* 26379–326392.

Jones, A., Roberts, D.L., Woodage, M.J., and Johnson, C.E. 2001. Indirect sulphate aerosol forcing in a climate model with an interactive sulphur cycle. *J. Geophys. Res. Atmos., 106,* 20293–310.

Jones, G., Fortescue, D., King, S., Williams, G., and Wright, S. 2010. Dimethylsulphide and dimethylsulphoniopropionate in the South-West Indian Ocean sector of East Antarctica from 30 degrees to 80 degrees E during BROKE-West. *Deep-Sea Research Part II – Topical Studies in Oceanography, 57,* 863–76 DOI: 10.1016/j.dsr2.2009.01.003.

Kettle, A.J. and Andreae, M.O. 2000. Flux of dimethylsulfide from the oceans: a comparison of updated data sets and flux models. *J. Geophys. Res., 105,* 26793–808.

Kettle, A.J., Andreae, M.O., Amouroux, D., Andreae, T.W., Bates, T.S., Berresheim, H., and Boniforti, R. 1999. A global database of sea surface dimethylsulfide (DMS) measurements and a procedure to predict sea surface DMS as a function of latitude, longitude and month. *Global Biogeochem. Cycles, 13,* 399–444.

Kloster, S., Dentener, F., Feichter, J., Raes, F., Lohmann, U., Roeckner, E., and Fischer-Bruns, I. 2010. A GCM study of future climate response to aerosol pollution reductions. *Clim. Dyn., 34,* 1177–94, DOI: 10.1007/s00382-009-0573-0.

Kloster, S., Six, K.D., Feichter, J., Maier-Reimer, E., Roeckner, E., Wetzel, P., and Esch, M. 2007. Response of dimethylsulfide (DMS) in the ocean and atmosphere to global warming. *J. Geophys. Res., 112,* DOI: 10.1029/2006jg000224.

Korhonen, H., Carslaw, K.S., Spracklen, D.V., Mann, G.W., and Woodhouse, M.T. 2008. Influence of oceanic dimethyl sulfide emissions on cloud condensation nuclei concentrations and seasonality over the remote Southern Hemisphere oceans: A global model study. *J. Geophys. Res. Atmos., 113,* DOI: D15204 10.1029/2007jd009718.

Lana, A., Bell, T.G., Simo, R., Vallina, S.M., Ballabrera-Poy, J., Kettle, A.J., and Liss, P.S. 2011. An updated climatology of surface dimethlysulfide concentrations and emission fluxes in the global ocean. *Global Biogeochemical Cycles, 25,* DOI: Gb1004 10.1029/2010gb003850.

Leck, C., Bigg, E.K., Covert, D.S., Heintzenberg, J., Maenhaut, W., Nilsson, E.D., and Wiedensohler, A. 1996. Overview of the atmospheric research programme during the International Arctic Ocean Expedition of 1991 (IAOE–91) and its scientific results. *Tellus, 48B,* 136–55.

Liss, P.S., Hatton, A.D., Malin, G., Nightingale, P.D., and Turner, S.M. 1997. Marine sulphur emissions. *Phil Trans. R. Soc. Lond. B. Biol. Sci., 352,* 159–69.

Lohmann, U., Feichter, J., Chuang, C.C. and Penner, J.E. 1999. Prediction of the number of cloud droplets in the ECHAM GCM. *J. Geophys. Res., 104,* 9169–98.

Lohmann, U., Rotstayn, L., Storelvmo, T., Jones, A., Menon, S., Quaas, J. and Ruedy, R. 2010. Total aerosol effect: radiative forcing or radiative flux perturbation? *Atmos. Chem. Phys., 10,* 3235–46.

Malin, G. 1997. Sulphur, climate and the microbial maze. *Nature, 387,* 857–9.

Menon, S., DelGenio, A.D., Koch, D. and Tselioudis, G. 2002. GCM simulations of the aerosol indirect effect: Sensitivity to cloud parameterisation and aerosol burden. *J. Atmos. Sci., 59,* 692–713.

Nightingale, P.D., Malin, G., Law, C.S., Watson, A.J., Liss, P.S., Liddicoat, M.I. and Upstill-Goddard, R.C. 2000. In situ evaluation of air-sea gas exchange parameterisations using novel conservative and volatile tracers. *Global Biogeochemical Cycles, 14,* 373–87.

O'Dowd, C.D., Lowe, J.A. and Smith, M.H. 1999. Coupling sea-salt and sulphate interactions and its impact on cloud droplet concentration predictions. *Geophys. Res. Lett., 26,* 1311–4.

O'Dowd, C.D., Smith, M.H., Consterdine, I.E. and Lowe, J.A. 1997. Marine aerosol, sea-salt, and the marine sulphur cycle: A short review. *Atmospheric Environment, 31,* 73–80.

O'Farrell, S.P. 1998. Investigation of the dynamic sea-ice component of a coupled atmosphere sea-ice general circulation model. *J. Geophys. Res., 103,* 15751–82.

Orellana, M.V., Matrai, P.A., Leck, C., Rauschenberg, C.D., Lee, A.M. and Coz, E. 2011. Marine microgels as a source of cloud condensation nuclei in the high Arctic. *Proceedings of the National Academy of Sciences of the United States of America, 108,* 13612–7 DOI: 10.1073/pnas.1102457108.

Parmesan, C. 2006. Ecological and evolutionary responses to recent climate change. *Annual Review of Ecology Evolution and Systematics, 37,* 637–69.

Pirjola, L., O'Dowd, C.D., Brooks, I.M. and Kulmala, M. 2000. Can new particle formation occur in the clean marine boundary layer? *J. Geophys. Res. Atmos., 105,* 26531–46.

Qu, B. and Gabric, A.J. 2010. Using genetic algorithms to calibrate a dimethylsulfide production model in the Arctic Ocean. *Chinese Journal of Oceanology and Limnology, 28,* 573–82, DOI: 10.1007/s00343-010-9062-x.

Quinn, P.K. and Bates, T.S. 2011. The case against climate regulation via oceanic phytoplankton sulphur emissions. *Nature, 480,* 51–6, DOI: 10.1038/nature10580.

Rasch, P.J., Crutzen, P.J. and Coleman, D.B. 2008. Exploring the geoengineering of climate using stratospheric sulfate aerosols: The role of particle size. *Geophys. Res. Lett., 35,* DOI: L02809/10.1029/2007gl032179.

Rotstayn, L.D. 1997. A physically based scheme for the treatment of stratiform clouds and precipitation in large-scale models .1. Description and evaluation of the microphysical processes. *Q. J. R. Meteorol. Soc., 123,* 1227–82.

Rotstayn, L.D., Cai, W.J., Dix, M.R., Farquhar, G.D., Feng, Y., Ginoux, P. and Wang, M.H. 2007. Have Australian rainfall and cloudiness increased due to the remote effects of Asian anthropogenic aerosols? *J. Geophys. Res. Atmos., 112,* DOI: D09202 Artn d09202.

Rotstayn, L.D. and Lohmann, U. 2002. Simulation of the tropospheric sulfur cycle in a global model with a physically based cloud scheme. *J. Geophys. Res., 107,* doi:10 1029/2002JD002128.

Schwartz, S.E., Charlson, R.J., Kahn, R.A., Ogren, J.A. and Rodhe, H. 2010. Why Hasn't Earth Warmed as Much as Expected? *J. Clim., 23,* 2453–64, DOI: 10.1175/2009jcli3461.1.

Serreze, M.C. and Francis, J.A. 2006. The arctic amplification debate. *Climatic Change, 76,* 241–64.

Shaw, G.E. 1983. Bio-controlled thermostasis involving the sulphur cycle. *Climate Change, 5,* 297–303.

Simó, R. and Dachs, J. 2002. Global ocean emission of dimethylsulfide predicted from biogeophysical data. *Global Biogeochemical Cycles, 16,* doi:1029/2001GB001829.

Smith, S.J., Pitcher, H. and Wigley, T.M.L. 2001. Global and regional anthropogenic sulfur dioxide emissions. *Global and Planetary Change, 29,* 99–119, DOI: 10.1016/s0921-8181(00)00057-6.

Spiro, P.A., Jacob, D.J. and Logan, J. A. 1992. Global inventory of sulfur emissions with 1x1 deg resolution. *J. Geophys. Res., 97,* 6023–36.

Tsigaridis, K., Krol, M., Dentener, F.J., Balkanski, Y., Lathiere, J., Metzger, S. and Kanakidou, M. 2006. Change in global aerosol composition since preindustrial times. *Atmospheric Chemistry and Physics, 6,* 5143–62.

Twomey, S. 1991. Aerosols, clouds and radiation. *Atmospheric Environment, 25,* 2435–42.

Vallina, S.M. and Simo, R. 2007. Strong Relationship Between DMS and the Solar Radiation Dose over the Global Surface Ocean. *Science, 10,* 506–8.

Vallina, S.M., Simo, R. and Gasso, S. 2006. What controls CCN seasonality in the Southern Ocean? A statistical analysis based on satellite-derived chlorophyll and CCN and model-estimated OH radical and rainfall. *Global Biogeochemical Cycles, 20.*

Vallina, S.M., Simo, R. and Manizza, M. 2007. Weak response of oceanic dimethylsulfide to upper mixing shoaling induced by global warming. *Proceedings of the National Academy of Sciences of the United States of America, 104,* 16004–9, DOI: 10.1073/pnas.0700843104.

Vaughan, N.E. and Lenton, T.M. 2011. A review of climate geoengineer-

ing proposals. *Climatic Change, 109,* 745–90, DOI: 10.1007/s10584-011-0027-7.

Watterson, I.G. 1997. The diurnal cycle of surface air temperature in simulated present and doubled CO_2 climates. *Clim. Dyn., 13,* 533–45 DOI: 10.1007/s003820050181.